IEEE Access
Multidisciplinary ⋮ Rapid Review ⋮ Open Access Journal

Received September 2, 2021, accepted September 14, 2021, date of publication September 15, 2021,
date of current version September 24, 2021.

Digital Object Identifier 10.1109/ACCESS.2021.3113167

Partial Interference Suppression in Massive MIMO Systems: Taxonomy and Experimental Analysis

ANDREA P. GUEVARA[1], (Graduate Student Member, IEEE), CHENG-MING CHEN[1], ALESSANDRO CHIUMENTO[2], (Member, IEEE), AND SOFIE POLLIN[1], (Senior Member, IEEE)

[1]ESAT, KU Leuven, 3001 Leuven, Belgium
[2]Faculty of Electrical Engineering, University of Twente, 7500 AE Enschede, The Netherlands

Corresponding author: Andrea P. Guevara (aguevara@esat.kuleuven.be)

This work was supported by the European Union's Horizon 2020 through the Machine Learning-Based, Networking and Computing Infrastructure Resource Management of 5G and Beyond Intelligent Networks (MARSAL) Project under Grant 101017171, through the REsilient INteractive applications through hyper Diversity in Energy Efficient RadioWeaves technology (REINDEER) Project under Grant 101013425, and through the Fonds Wetenschappelijk Onderzoek Excellence of Science (FWO EOS) Project MUSE-WINET.

ABSTRACT Densely deploying Massive MIMO access points results eventually in cell-free systems. To achieve scalability, users should be allocated only to neighbouring access points as it is not realistic to assume that all access points serve all users. At the same time interference from other nearby users should be suppressed, as it is not practical to suppose that channel state information from all users is available for full MMSE-based interference suppression. Motivating the use of partial MMSE combining vectors. This work shows the taxonomy of proposed MMSE combining vectors for different clustering techniques, and three approaches to partially suppress interference based on 1) interferers with common access points, 2) strongest channel gain and 3) strongest eigendirections. In order to analyse the pros and cons of the three interference suppression methods, a general parameterised MMSE combining vector is proposed, that is generic enough to represent any clustering methodology and any partial interference suppression technique. The results are presented in terms of spectral efficiency and computational cost, with the aid of a dense indoor massive MIMO experiment and contrasted with an indoor simulation using the WINNER II channel model. Experimental and simulation results show that partial suppression based on shared access points is not suitable for systems with a small probability of users sharing the serving access points, as dominant interference is likely to come also from users connected to access points not serving the harmed user. Channel gain based interference suppression provides the best controllable approach in terms of spectral efficiency and computational cost. However, eigendirections-based interference suppression achieves the highest spectral efficiency, when the number of antennas per access point is high enough.

INDEX TERMS Massive MIMO, interference cancellation, MMSE combining vector, user-centric, network-centric, cell-free.

I. INTRODUCTION

The number of wireless users with demanding communication requirements has increased abruptly over time, saturating the scarce spectrum for broadband communications. Nevertheless, with the deployment of a large number of antennas in a base station, it is possible to implement spatial multiplexing and transmit precoding or receive combining, allowing simultaneous communication between multiple users using the same bandwidth. These techniques are implemented in Massive MIMO systems which have demonstrated the increase of spectral efficiency, both theoretically [1]–[3] and experimentally [4]–[11].

In a Massive MIMO system, during uplink transmission, the base station receives at the same time multiple signals sent from different users. A combining vector is applied to estimate the signal of each user individually. This combining vector could reject the signals from the undesired users

The associate editor coordinating the review of this manuscript and approving it for publication was Liang Yang.

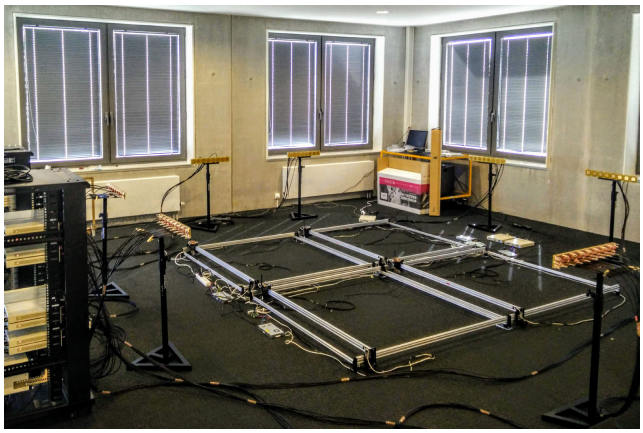

FIGURE 1. KU Leuven Massive MIMO testbed deployed in an indoor scenario. The base station antennas are distributed around the mobile station antennas located on the XY positioners on the ground. This experiment gathered the channel information from more than 250K user locations.

and suppress the noise. Traditional state-of-the-art techniques have been widely studied, such as Maximum Ratio (MR), Zero Forcing (ZF), Regularized Zero Forcing (R-ZF) and Minimum Mean Squared Error (MMSE) combining vectors.

This work focuses on MMSE, which maximizes the SINR while reducing the minimum squared error between the desired received signal and the processed received signal [12]. With MMSE and under the assumption of linearly independent user correlation matrices, the spectral efficiency and capacity in a massive MIMO system can, in theory, increase without limit [13]. Therefore, MMSE is known as the optimal linear combining vector [12].

Still, MMSE comes at a high computational cost, scaling with the total number of users and antennas in the system, and under unrealistic assumptions, the channel state information (along with channel estimation errors) from all users must be known in advance by all base stations in the system.

The implementation of partial combining vectors has the potential to reduce the computational cost at small spectral efficiency cost. The ''partial'' name implies the interference cancellation of only a subset of users (while the optimal MMSE combining vector suppresses the interference of all users) [14], [15]. A complete overview of the selection of the subset of suppressed users in a partial combining vector is described below.

A. MOTIVATION AND RELATED WORK

Different interference suppression approaches lead to a variety of partial combining vectors; however, the implementation of those depends directly on the user allocation or clustering technique of the system. Here we will discuss three clustering techniques:

1) During the introduction of massive MIMO, the concept of cells was applied for clustering; this approach is also known as *network-centric*. It means that a single massive MIMO base station serves one cell or sector, using the traditional cellular network topology. In this case, the interference from users within the same cell was categorised as intra-cell interference, while inter-cell interference comes from users in any other cell. Here we can find three combining vectors: First, the optimal MMSE combining vector, named Multi-cell MMSE (M-MMSE) which suppresses the interference from all users in the system (intra and inter-cell interference). Second, a Partial Multi-cell MMSE (PM-MMSE) which suppresses intra-cell and partial inter-cell interference, the selection of the partial interference in this combining vector is for instance based on the wireless channel gain between users in other cells and the analysed cell [8]. Third, a combining vector which only suppresses intra-cell interferers, named as Single-cell MMSE (S-MMSE). This combining vector can also be classified as partial MMSE as the suppressed users are those that ''share'' the same base station [2].
2) Nowadays, a *user-centric* topology has been proposed for dense massive MIMO systems, also referred as a scalable cell-free network [23]. In this case, each user is served by multiple cooperating base stations (a.k.a access points[1]). Similar to the *network-centric* case, an optimal full MMSE combining vector suppresses interference from all users in the system towards the set of access points that serve a particular user. For this topology, a partial MMSE combining vector named P-MMSE [15] is introduced to suppress only interference from users that are served by the same set of access points as the reference user.
3) The extension of the previous scalable user-centric topology leads to a *fully distributed cooperative* system, known also as cell-free, where all the access points serve all the users. Here the optimal MMSE suppresses the interference from all the users towards all the antennas. As a partial combining vector, a Large Scale Fading Decoding (LSFD) is introduced in [17] where the suppression of interference for a particular user relies on the selection of a subset of the closest users. This selection is based on the channel gain, named here as large scale fading.

To summarise the different clustering strategies, Table 1 provides an overview of the different combining vectors categorised under multiple techniques of interference suppression.

Partial interference suppression has also been implemented in ZF combining vectors. The taxonomy for this combining vector is additionally presented in Table 1. The main difference with MMSE is that ZF does not consider channel estimation errors and for optimal performance, the joint number of antennas from the access points must be higher than the number of users to be served. Interestingly, we can notice that ZF and MMSE have similar techniques for partial suppression

[1]The difference between base station and access point it is that the first one processes the data locally, while the second one can rely on an external CPU.

TABLE 1. Combining vectors (and precoders) taxonomy for full and threepartial interference suppression methods and three clustering strategies. The state-of-the-art combining vectors that are analysed in this paper appear in slightly shaded cells, for essentially three network topologies. While the new combinations analysed in this paper appear in light blue. Note that we will use our naming convention P-MMSE-S/G/E in the remainder of the paper, and not the state-of-the-art naming.

Combining Vector	Interference Suppression	Suppression Method	Network-centric	User-centric	Fully Cooperative
MMSE	Total	MMSE	M-MMSE [16]	MMSE [15]	MMSE [15]
	Partial	Shared access points based (P-MMSE-S)	S-MMSE [12]	P-MMSE [15]	This work
		Channel gain based (P-MMSE-G)	PM-MMSE [14]	This work	LSFD [17]
		Eigen direction based (P-MMSE-E)	This work	This work	This work
ZF	Total		-	-	F-ZF [18]
	Partial	Shared access points based	ZF [2]	PZF [19]	-
		Channel gain based	P-ZF [20], ZF-LSFD [21]	-	PZF [18]
		Eigen direction based	ZF-EDA [22]	-	-

based on shared access points and channel gains. However, in [22], a new interference suppression method is introduced only for ZF and for a network-centric scenario. In this case, the interference suppression is towards the strongest eigendirections of users located in other cells. To the best of our knowledge, this interference suppression technique has not been yet considered in a partial MMSE combining vector, regardless of the clustering method.

In Table 1, we also introduce the naming convention we will further use in this paper for the full MMSE and partial combining vectors P-MMSE-S, P-MMSE-G, and P-MMSE-E. We will compare them for multiple network topologies going from traditional network-centric (multi-cell Massive MIMO), to user-centric (scalable cell-free) and fully cooperative (cell-free) topologies. All studied cases are highlighted in the table in blue.

B. CONTRIBUTION

The main goal of this work is the analysis of the multiple interference suppression techniques in a partial MMSE combining vector. This analysis is applied to a system with the three clustering strategies: network-centric, user-centric and fully cooperative clustering.

To understand the advantages and disadvantages of each partial suppression method this work provides the following contributions:

- A literature review of the methods for partial interference suppression (MMSE and ZF combining vectors). Those methods are classified according to three clustering strategies and presented in Table 1. In this taxonomy, we realize that partial interference suppression based on eigendirections has not been studied yet in MMSE. Therefore, we include the analysis of eigendirections suppression in MMSE combining vector as part of the partial suppression techniques. Interestingly, it is shown that it outperforms the state-of-the-art methods for scenarios where there are sufficient active antennas per access point.
- Proposal of a single MMSE combining vector that can be applied to any clustering technique. This combining vector is parameterised to represent any of the three interference suppression methods given in Table 1.
- The analysis between the different suppression methods and clustering strategies is carried out experimentally, with the aid of the KU Leuven Massive MIMO testbed and contrasted with simulations using the WINNER II channel model in a similar scenario. Although this model is spatially non-consistent and does not support the evaluation of very dense environments, we show that this channel model provides a spectral efficiency approximation for a simulated scenario that mimics the measurement environment.

The analysis of this work relies on a Massive MIMO system with time division duplex (TDD) mode. The measured channel database collected in the experiment is available.[2]

C. PAPER OUTLINE

The rest of the paper is organised as follows. In Section II the system model for different clustering strategies is introduced, along with the channel estimation and uplink data processing. Section III introduces the proposed MMSE combining vector, and the three different methods to partially suppress interference. Section IV describes the computational complexity to process the data per combining vector. The evaluated scenarios, data collection and processing used to analyse the proposed combining vectors is presented in Section V. The results and main findings are presented in Section VI and Section VII states the conclusions of this work.

D. NOTATION

The following notations are used in this paper: $\mathbf{x} \in \mathbb{C}^M$ represents an M $\times$ 1 complex vector, $\mathbf{X} \in \mathbb{C}^{M \times N}$ is an M$\times$N complex matrix. $\mathbf{x}^H$ and $\mathbf{x}^T$ represents the transpose and conjugate-transpose of vector $\mathbf{x}$. $||\mathbf{x}||$ is the Euclidean norm of $\mathbf{x}$. $\mathbb{E}\{\mathbf{x}\}$ is the expectation of $\mathbf{x}$. $\mathbb{V}\{\mathbf{x}\}$ is the variance of $\mathbf{x}$.

II. SYSTEM MODEL

The analysis of this work relies on an uplink massive MIMO wireless system with time division duplex (TDD) mode. This system has set of $\mathcal{K}$ users, and $\mathcal{L}$ access points, each of the access points has a set of $\mathcal{N}$ number of antennas. A subset $\mathcal{S}$

[2]https://homes.esat.kuleuven.be / sdebast/measurements/measurements _ boardroom.html

of access points, $\mathcal{S} \subset \mathcal{L}$ serves each user. The cardinality of each set and subset, is given as: $K = |\mathcal{K}|$, $L = |\mathcal{L}|$, $N = |\mathcal{N}|$ and $S = |\mathcal{S}|$.

In this way the wireless channel between user k and all the antennas that belong to the subset of access points that serve this user $\mathcal{S}_k$ is given as a vector $\mathbf{h}_k$ with a size of N times S_k, $\mathbf{h}_k \in \mathbb{C}^{NS_k}$, where $S_k = |\mathcal{S}_k|$. In this work we assume that all the users transmit with the same uplink power p.

A. NETWORK MANAGEMENT AND CLUSTERING STRATEGIES

For a massive MIMO system, multiple forms of clustering methods between users and access points have been studied in [9], [15], [19], [23], [24]. Those methods range from a fully distributed cooperative system to a system comprised of small cells. In addition to user allocation decisions, the distributed Massive MIMO system should also decide where the signals are processed. In [24], the data processing for those systems are classified into multiple levels: Level 4 focuses on fully central processing, and Level 1 focuses on fully local processing. Our taxonomy does not include data processing but instead focuses on the assignment of access points to users.

1) FULLY COOPERATIVE CLUSTERING

This is the extreme distributed massive MIMO system case (aka. cell-free), where all the access points cooperate with a single central processing unit (CPU) [25]. In this fashion, all the users are served simultaneously by all the antennas deployed on the system. Therefore, for each user k in the system, $S_k = L = 1$ and all the antennas serve all the users.

So far, this topology has been proven theoretically as the one to provide the highest performance. However, it carries a high cost as it requires unlimited capacity at the backhaul as the payload increases with the number of access points. For this case, uplink data transmission (combining vector) and downlink data transmission (precoder), are carried out in the centralised CPU. Moreover, it requires a high computational cost which is a function of the total number of antennas and users deployed in the system.

2) USER-CENTRIC CLUSTERING

An option to reduce not only the signal traffic but the computational cost in a fully cooperative system is with the user-centric approach. Essentially, each user is served by more than one access point; the clustering is based on the strongest channel gain [23]. So, for user k, $1 < S_k < L$.

Each access point carries out the channel estimation procedure locally. However, the subset of access points that serve each user must coordinate to perform each combining vector and precoding during uplink and downlink data transmission, respectively. This coordination can be done with the distribution of CPUs to control a set of access points as it is presented in [15]. A broad explanation of the signal processing for this level of cooperation can be found in [24]. As the number of antennas serving a user is smaller in comparison with the fully cooperative case, the computational cost for combining vector and precoding is reduced.

3) NETWORK-CENTRIC CLUSTERING

This is a particular topology where each access point selects a set of users to be served based on the channel gain. The main difference with the user-centric case is that each user is served only by a single access point. Thus, for all users k, $S_k = 1$. This topology has been widely studied as the system access points are distributed in cells, and interference is treated as intra-(users served by the same cell) or inter-cell (users served by any other cell).

For this particular case, there is no cooperation between access points for channel estimation, uplink and downlink transmission, so every process is carried out locally in each access point. Therefore there is a massive reduction in the data transmission at the backhaul. Additionally, the computation complexity is highly reduced as it depends only on N.

B. CHANNEL ESTIMATION

The Channel State Information (CSI) is the set of channel response realisations known by any access point. To obtain the CSI, a channel estimation process is required. During uplink training, an orthogonal pilot sequence $\mathbf{\Phi}_k$ with length τ_p[3] is allocated to each user k. If all the users have a unique orthogonal pilot sequence, then this is a system without pilot contamination. This condition is assumed in this work.

Once all the transmitted pilots arrive simultaneously to the different access points, the channel estimation function decorrelates each user's channel by multiplying the received signal with the conjugate of each pilot sequence. Each decorrelated signal will be then used as the input information to the MMSE channel estimation given by Theorem 3.1. from [12]. Every access point carries out this process for each user in the system, including those users that are served by this access point and those users which do not belong to it. The knowledge of the channel estimation of the latter ones is used to suppress the interference, described in the next section.

The estimated channel per user k to all the antennas in the subset of access points $\mathcal{S}_k$ is given as $\hat{\mathbf{h}}_k^{\mathcal{S}_k} \in \mathbb{C}^{NS_k}$. Thus, the channel estimation error is represented as

$$\tilde{\mathbf{h}}_k^{\mathcal{S}_k} = \mathbf{h}_k^{\mathcal{S}_k} - \hat{\mathbf{h}}_k^{\mathcal{S}_k}. \tag{1}$$

In the same way, the correlation error matrix of the channel estimation error between user k and its serving access points is given as $\mathbf{C}_k \in \mathbb{C}^{NS_k \times NS_k}$, and is obtained as:

$$\mathbf{C}_k^{\mathcal{S}_k} = \mathbb{E}\left\{ \left(\mathbf{h}_k^{\mathcal{S}_k} - \hat{\mathbf{h}}_k^{\mathcal{S}_k}\right)\left(\mathbf{h}_k^{\mathcal{S}_k} - \hat{\mathbf{h}}_k^{\mathcal{S}_k}\right)^H \right\}. \tag{2}$$

Considering user k as the reference user. The channel estimation matrix for all the users K to the subset of access points $\mathcal{S}_k$ (the users can be served or not by $\mathcal{S}_k$) as:

$$\hat{\mathbf{H}}^{\mathcal{S}_k} = \left[\hat{\mathbf{h}}_1^{\mathcal{S}_k} \ldots \hat{\mathbf{h}}_k^{\mathcal{S}_k} \ldots \hat{\mathbf{h}}_K^{\mathcal{S}_k}\right]. \tag{3}$$

[3] τ_p uplink data samples per coherence block are used to transmit a pilot sequence.

C. UPLINK TRANSMISSION

After channel estimation and during uplink transmission, user k sends over its channel a data signal d_k to the subset of access points $\mathcal{S}_k$. Simultaneously, the remaining $i\,(i \neq k)$ users in the system also transmit uplink signals (d_i) creating interference to d_k.

The received signals plus noise are combined and received by $\mathcal{S}_k$ as $\mathbf{y}^{\mathcal{S}_k} \in \mathbb{C}^{NS_k}$. It is worth emphasising that the desired uplink signal d_k, will be received at $\mathcal{S}_k$ over the estimated and residual error channels as follows:

$$\mathbf{y}^{\mathcal{S}_k} = \underbrace{\hat{\mathbf{h}}_k^{\mathcal{S}_k} d_k}_{\text{Estimated channel}} + \underbrace{\tilde{\mathbf{h}}_k^{\mathcal{S}_k} d_k}_{\text{Channel error}} + \underbrace{\sum_{\substack{i=1 \\ i\neq k}}^{K-1} \mathbf{h}_i^{\mathcal{S}_k} d_i}_{\text{Interference}} + \underbrace{\mathbf{n}}_{\text{Noise}}. \tag{4}$$

Note that in the previous equation the interference term is represented as the signal from all the other users in the system (either served by $\mathcal{S}_k$ or not). The interference is then classified in two sets of interference. This interference classification is important for the application of a partial combining vector. On the one hand, there is a subset of $\mathcal{Q}$ interferes, with cardinality $Q = |\mathcal{Q}|$ called *"dominant interferes"* that will be selected based on different criteria for suppression, described in detail in the next section. On the other hand, the remaining subset $\mathcal{R}$, with cardinality $R = |\mathcal{R}|$ is considered as *"minor interferes"*. Therefore, the interference term in (4) is given by:

$$\sum_{\substack{i=1 \\ i\neq k}}^{K-1} \boldsymbol{h}_i^{\mathcal{S}_k} s_i = \sum_{q\neq k}^{Q} \boldsymbol{h}_q^{\mathcal{S}_k} s_q + \sum_{r\neq k}^{R} \boldsymbol{h}_r^{\mathcal{S}_k} s_r. \tag{5}$$

Once the received signal $\mathbf{y}^{\mathcal{S}_k}$ arrives at the $\mathcal{S}_k$ access points, the state-of-the-art provides multiple techniques called combining vectors ($\mathbf{v}_k$) to detect the desired signal d_k of each user. Each combining vector deals differently with the signal components in (4). So, *Maximum-Ratio* (MR) [26] increases the power of the desired signal but does not suppress either interference or noise. In the case of *Zero-Forcing* (ZF) [27] and *Regular Zero-Forcing* (RZF), interference is nullified as well as noise when RZF is applied. Nevertheless, the *Minimum-Mean Squared Error* (MMSE) [16] combining vector cancels interference, channel errors and noise from the received signal.

III. MMSE AND PARTIAL MMSE (P-MMSE) COMBINING VECTORS

Variations of the MMSE combining vector have been widely studied (see Table 1). When the interference from all the users in the system is suppressed, then the MMSE combining vector is considered as the "*optimal*" solution, but it requires a higher computational cost. Therefore, to reduce this cost, the P-MMSE combining vector had been proposed which suppress only the "*dominant interferers*".

The proposed generic representation of MMSE or P-MMSE combining vector representation to estimate d_k in (4) is given by:

$$\mathbf{v}_k = p\left(\mathbf{Z}_k^{\mathcal{S}_k}\mathbf{P}\left(\mathbf{Z}_k^{\mathcal{S}_k}\right)^H + \sum_{i=1}^{K} p\mathbf{C}_i^{\mathcal{S}_k} + \sigma_{UL}^2\mathbf{I}_{NS_k}\right)^{-1}\hat{\mathbf{h}}_k. \tag{6}$$

From the previous equation, we can notice that this unified combining vector is versatile enough to be used in any clustering technique ($\mathcal{S}_k$ term). While the $\mathbf{Z}_k^{\mathcal{S}_k}$ term represents the full or partial interference suppression, explained in details below.

In the same equation, $\mathbf{P} = p\mathbf{I}_{Q+1}$, represents the matrix of the transmitted power. Here $\mathbf{I}_{Q+1}$ and $\mathbf{I}_{NS_k}$ are identity squared matrices of order $Q+1$ and NS_k, respectively. While σ_{UL}^2 is the noise variance obtained through the system signal-to-noise-ratio (SNR). Finally, $\mathbf{Z}_k \in \mathbb{C}^{NS_k \times Q+1}$ represents the subset of Q wireless channels to be suppressed, including the wireless channel of the required user k.

Notice that the processing of (6) is done jointly across all serving access points $\mathcal{S}_k$. And according to the selection of interference suppression, there are two types of combining vectors:

1) MMSE

Suppress the interference from all the users in the system. As:

$$\mathbf{Z}_k^{\mathcal{S}_k} = \hat{\mathbf{H}}^{\mathcal{S}_k}. \tag{7}$$

So all the interferes are considered as dominant, $Q = K-1$ and $R = 0$.

2) P-MMSE

In this case the suppression of the interference is carried out only to the "*dominant interferes*", while the "*minor interferes*" are considered as noise. Thus, $Q < K$ and $k \notin \mathcal{Q}$. Therefore:

$$\mathbf{Z}_k^{\mathcal{S}_k} = [\hat{\mathbf{h}}_k^{\mathcal{S}_k} \quad \hat{\mathbf{h}}_1^{\mathcal{S}_k} \ldots \hat{\mathbf{h}}_q^{\mathcal{S}_k} \ldots \hat{\mathbf{h}}_Q^{\mathcal{S}_k}]. \tag{8}$$

The selection of the subset $\mathcal{Q}$ considered in this work is classified based on three approaches. Therefore, an additional letter **S**, **G** or **E** will be added to $\mathcal{Q}$ and Q to differentiate the method used:

- **P-MMSE-S** (P-MMSE-Shared access points Based Suppression): This method is proposed in [15], and suppress the interference generated by users that are served at least by one of the access points ($\mathcal{S}_k$). It is important to mention that the selected dominant interferers $\mathcal{Q}_S$ in (8), can not be altered as $\mathcal{Q}_S$ is fixed during the user and access point allocation procedure or clustering.
- **P-MMSE-G** (P-MMSE-Gain Based Suppression): This method relies on the channel gain between all users in the system i, $i \neq k$ and the subset of access points that served the desired user k ($\mathcal{S}_k$). So, the channel gain is defined as:

$$\beta_i^{\mathcal{S}_k} = \mathbb{E}\{||\mathbf{h}_i^{\mathcal{S}_k}||^2\}. \tag{9}$$

Once the channel gain of all users is estimated, those are ordered in descending order. Then the $\mathcal{Q}_G$ channels with

the highest channel gain are included in (8). The set of Q_G users are known as the *dominant interferes*.
It is important to note a correlation between the Shared and Gain based methods as the clustering of the users to the access points depend on their β.

- **P-MMSE-E** (P-MMSE-Eigendirection Based Suppression): This method uses the singular value decomposition (SVD) on $\hat{\mathbf{H}}^{\mathcal{S}_k}$. Then the Q_E left singular vectors $\mathbf{u}_{q_E}^{\mathcal{S}_k} \in \mathbb{C}^{NS}$ are selected. Those vectors correspond to the eigenvalues that are sorted previously in a descendent order. In this way the matrix $\mathbf{Z}_k$ is given by:

$$\mathbf{Z}_k^{\mathcal{S}_k} = [\hat{\mathbf{h}}_k^{\mathcal{S}_k} \quad \mathbf{u}_1^{\mathcal{S}_k} \dots \mathbf{u}_{q_E}^{\mathcal{S}_k} \dots \mathbf{u}_{Q_E}^{\mathcal{S}_k}]. \tag{10}$$

As this method relies on the SVD of $\hat{\mathbf{H}}^{\mathcal{S}_k}$ then $Q_E \leq NS_k$. When this condition is not guaranteed , and the algorithm wants to suppress more directions than we can find in the system, then $\mathbf{Z}_k$ considers all the eigendirections.
A similar method is used for the ZF-EDA combining vector presented in [22]. However, the presented method is adapted to a P-MMSE combining vector which considers channel estimation errors and the noise variance.

It is worth mentioned that in [14], [15] the correlation error matrix $\left(\mathbf{C}_i^{\mathcal{S}_k}\right)$ considers only the suppressed users, $i \in Q$, see (6). In contrast, our proposed combining vector selects all users in the system $i \in K$, which allows a fair comparison between the three interference suppression techniques presented above. As in the P-MMSE-E case, due to the SVD decomposition, it is not possible to identify the channel of the "*dominant interferers*" but only dominant eigendirections.

The same principle from the correlation error matrix is applied to the power matrix $\mathbf{P}$ in (6), as it is assumed that all the users transmit at the same power.

Remark: In the case that each user has M antennas, MK data streams can be estimated independently with (6). Increasing the number of antennas per user improves the spectral efficiency only when the number of antennas per access point is large enough to achieve the multiplexing capabilities of the system [28].

A. SINR AND UPLINK SPECTRAL EFFICIENCY

After multiplying the received signal in (4) with any combining vector $\mathbf{v}_k$, Theorem 4.1 in [12] proposes an instantaneous SINR of the k user (under the assumption that MMSE is used as channel estimation), as follows:

$$SINR_k = \frac{p|\mathbf{v}_k^H \hat{\mathbf{h}}_k^{\mathcal{S}_k}|^2}{\sum\limits_{\substack{i=1 \\ i\neq k}}^{K} p|\mathbf{v}_k^H \hat{\mathbf{h}}_i^{\mathcal{S}_k}|^2 + \mathbf{v}_k^H \left(\sum\limits_{i=1}^{K} p\mathbf{C}_i^{\mathcal{S}_k} + \sigma_{UL}^2 \mathbf{I}_{NS_k}\right)\mathbf{v}_k}. \tag{11}$$

Using the lower bounded capacity from the ergodic uplink as in [2], the spectral efficiency of user k is given by

$$\mathrm{SE}_k = \frac{\tau_u}{\tau_c} \mathbb{E}\left\{\log_2\left(1 + \mathrm{SINR}_k^{UL}\right)\right\}. \tag{12}$$

where τ_u/τ_c[4] is the portion per coherence block[5] used to transmit UL data.

IV. COMPUTATIONAL COST

The computational cost is quantified as the number of complex multiplications and divisions[6] required per coherence block to compute the desired signal vector. In [12] Lemmas B.1 and B.2 describe the number of complex multiplications required by each MMSE combining vector in (6).

First, $((NS_k)^2 + NS_k)(Q + 1)/2$ multiplications are required to compute a channel matrix with its conjugate transpose, $\mathbf{Z}_k^{\mathcal{S}_k}\mathbf{P}\left(\mathbf{Z}_k^{\mathcal{S}_k}\right)^H$. Second, the inverse term $(.)^{-1}$ of any MMSE combining vector requires $((NS_k)^3 - NS_k)/3$ complex multiplications. Finally, the cost of the mentioned inverse term and $\hat{\mathbf{h}}$ is $(NS_k)^2$ times. Thus, the total number of complex multiplications per coherence block includes $\tau_u NS_k K$ plus the complex multiplications shown in Table 2.

On the one hand, as all channel gains in the system are already estimated during user allocation, no extra complex multiplications are needed to computed (9) for PMMSE-S or PMMSE-G. On the other hand, the number of complex multiplications additional to the estimation of the SVD in P-MMSE-E is Q_E^2 based on [29].

V. PERFORMANCE EVALUATION

In this work, we used two approaches to evaluate the performance of the proposed partial combining vectors under different clustering techniques. The first method is a dense indoor massive MIMO experiment with the aid of the KU Leuven Massive MIMO testbed, and the second method is an indoor simulation using the WINNER II channel model.

[4] τ_u is the uplink data samples received per coherence block, and τ_c is the total number of samples per coherence block.
[5] A coherence block is the set of subcarriers and samples over time and frequency which its impulse response tends to be constant. [12].
[6] Additions and subtractions also contribute to the computational cost. However, their contribution is small and are neglected.

TABLE 2. Computational cost for each combining vector per user *k*.

Combining Vector	Complex Multiplications
MMSE	$\frac{(NS_k)^2+NS_k}{2}K + \frac{(NS_k)^3-NS_k}{3} + (NS_k)^2$
P-MMSE-S	$\frac{(NS_k)^2+NS_k}{2}(Q_S+1) + \frac{(NS_k)^3-NS_k}{3} + (NS_k)^2$
P-MMSE-G	$\frac{(NS_k)^2+NS_k}{2}(Q_G+1) + \frac{(NS_k)^3-NS_k}{3} + (NS_k)^2$
P-MMSE-E	$\frac{(NS_k)^2+NS_k}{2}(Q_E+1) + \frac{(NS_k)^3-NS_k}{3} + (NS_k)^2 + Q_E^2$

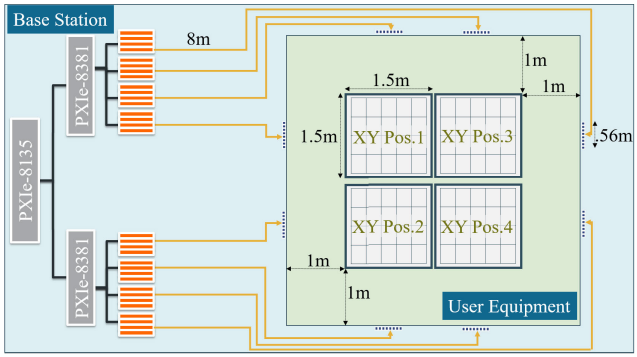

FIGURE 2. Massive MIMO LoS experimental scenario deployment for eight distributed ULA (D-ULA) antenna array.

A. MASSIVE MIMO EXPERIMENT

The KU Leuven massive MIMO testbed contains a 64-patch antenna base station and a set of single-antenna user equipments. One of the main characteristics of the 64-patch antennas at the base station is their modularity. During this experiment, we were able to deploy the antennas as a Distributed ULA (D-ULA). In this distributed scenario, we deployed homogeneously eight different arrays of 1×8 antennas around the outer ring of the XY positioners, as shown in Fig. 2.

In this experiment we use four XY positioners which hold a dipole antenna each. One universal software radio peripherals (USRPs) controls a pair of antennas transmitting independent data streams. In Fig. 2, USRP1 controls the antennas placed on XY positioners 1 and 3; and USRP2 the dipole antennas of XY positioners 2 and 4. This experiment emulates an indoor industrial scenario where transmitting nodes (or users) will be deployed on the ground in a grid distribution with a separation of 25 and 30 cm, as the one detailed in [30]. The distance between each array and the closest side of the positioners is 1 meter.

The positioners moved synchronously to 30 different positions each every 30 seconds, with simultaneous and continuous signal transmission. The received uplink signal, generated by the USRPs when halting on the pre-defined locations, was collected and processed by the massive MIMO base station for each of the 120 positions, and the channel for each position was saved to be processed offline. During the experiment, the base station is controlled in real-time by the LabVIEW Communications MIMO Application Framework 1.1. [31]. The transmit power for the 120 transmit positions was the same.

B. VIRTUAL CLUSTERING

During post processing data, the wireless channels collected for each of the 120 positions are treated as 120 virtual users. Similarly, the set of wireless channels corresponding to a set of single or adjacent antenna arrays are treated as virtual access points, according to $\mathcal{L}$.

Therefore, in the case of a single virtual access point, all the antenna arrays serve the set of selected users. For a system with two virtual access points ($L = 2$), four adjacent antenna arrays become one access point, thus, each access point has 32 antennas ($N = 32$). The virtualisation of the antenna arrays is carried out in the same way for systems with four virtual access point, as two adjacent arrays ($N = 16$). And eight virtual access points, where each antenna array is considered as a virtual access points ($N = 8$).

C. DATA PROCESSING

After channel collection, the experimental wireless channel ($\mathbf{h}_k^{\text{meas}}$) was processed offline. The first step was the normalization of the channel over all subcarries.

$$\mathbf{h}_k(f) = \frac{\mathbf{h}_k^{\text{meas}}(f)}{\sqrt{\sum_M |\mathbf{h}_k^{\text{meas}}(f)|^2}}. \tag{13}$$

The second step is the selection of the network type (values for L and S_k), followed by the allocation of the users to each access point based on the channel gain. In the third step the effective SNR is set to 20dB, in this way additional noise is added so MMSE channel estimation can be carried out. So the collected channel represents $\mathbf{H}$, and after MMSE it is possible to obtain $\hat{\mathbf{H}}$.

As a fourth step, MMSE and the variations of P-MMSE combining vectors are computed, concluding with the estimation of the spectral efficiency.

D. WINNER II SIMULATIONS

To determine a simulation-based channel model for the same indoor experimental scenario, we use the WINNER II toolbox in Matlab based on [32] to obtain the wireless channel between users deployed in random locations in an area of $3m^2$. To follow the minimum requirements for using this model as an indoor deployment, the antennas were placed at 3m from the closest users. This channel model considers the cross-correlation of large-scale fading such as shadowing, pathloss, Doppler, among others. For a stationary scenario, the variation between users is preferably ten wavelengths.

The propagation scenario considered is an indoor case, where the antenna arrays are located in the same position as in Fig. 2.

After obtaining the model-based channel, the user *transmit power* (p) is included according to the power set during the indoor experiment as 20dBm. Similarly, as was described in the previous section, the SNR is set to 20dB for the channel estimation process. Then, we obtain the spectral efficiency for the different P-MMSE combining vectors. The setting details using for the simulation is listed in Table 3.

After the simulation of the wireless channel, a virtual clustering is carried out for each system according to $\mathcal{L}$ and $\mathcal{S}$ as it was described in Sec. V-B.

VI. EXPERIMENTAL RESULTS

The results presented in this section consider 200 possible scenarios (every scenario represents a random set of $\mathcal{K}$ users), with $K = 32$ or 8. The following results use the data obtained

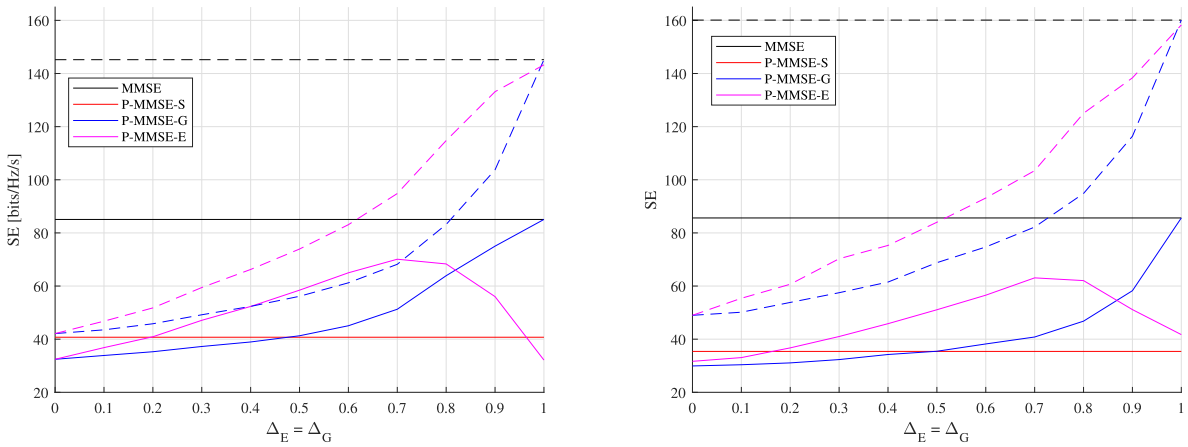

(a) Experimental results.

(b) Simulation results.

FIGURE 3. Variation of the sum spectral efficiency (SE) and the percentage of suppresed users: $\Delta_E \approx Q_E(L/K)$ and $\Delta_G \approx Q_G(L/K)$, where $\Delta_G = \Delta_E$, $K = 32$ and under two clustering strategies: 1) Dashed lines when $L = S = 1$. 2) Solid lines when $L = 2$ and $S = 1$. The results for experimental and simulation datasets show a similar SE performance between the different combining vectors. The P-MMSE-E combining vector outperforms in contrast with P-MMSE-S and P-MMSE-G, for a Δ_E given interval.

TABLE 3. Simulation settings used to simulated winner II wireless channels and its data processing.

Propagation scenario	A1 (Indoor office/residential)
Frequency	2.61GHz
Access pointantenna arrays	1-2-4-8
Number of antennas per array	8
Distance between antennas	0.4595m
Access point antenna array configuration	ULA
Number of users	8 - 32
Number of antennas per user	1
Shadowing model used	yes
Path model used	yes
User speed	0m/s
Number of samples	100
Number of wireless channels	64-256

by the Massive MIMO experiment (Section V-A) and the simulation mentioned above (Section V-D).

A. SUM SPECTRAL EFFICIENCY AND SUPPRESSED DOMINANT INTERFERERS

One of the decisive factors for interference suppression in any P-MMMSE combining vector is the selection of the adequate dominant interferers. In this subsection, we present a performance comparison between P-MMSE-G and P-MMSE-E when both suppress the same amount of users or eigendirections. The results are contrasted with the optimal MMSE and the P-MMSE-S.

For the experimental results Fig. 3 presents the total spectral efficiency of 32 users served by two clustering strategies: First, a fully cooperative case as $L = 1$, $S = 1$ (dashed lines). Second, a two-cell systems as $L = 2$, $S = 1$ (solid lines). The spectral efficiency varies as function of Q_E and Q_G, presented as the percentage of suppressed users $\Delta_E \approx Q_E(L/K)$ and $\Delta_G \approx Q_G(L/K)$. It is worth to emphasise that the number of users (K) are not allocated uniformly to the number of access points (L) but on average the previous approximations hold.

Although the ratio N/K between the number of antennas and users in both scenarios is the same, there are two main differences between the two clustering strategies. First, as it is expected for an MMSE combining vector, the full cooperative case (dashed lines) achieves a spectral efficiency which is almost twice that of the two-cell case (solid lines), due to the large number of antennas serving each user and the full interference suppression.

Second, when partial interference suppression is considered, one might expect that the suppression of users with a higher channel gain will increase the performance of the system (as most of the works assume in the state-of-the-art) rather than the suppression of eigendirections. However, in Fig. 3, it is interesting to see that P-MMSE-E has a better performance than P-MMSE-G in the fully cooperative scenario (dashed lines). This behaviour is similar in the two cell without collaboration case $L = 2$ and $S = 1$ (solid lines), when $\Delta_E = \Delta_G \leq 0.7$. After this saturation point, it is interesting to see that the suppression of more eigendirections (given by other users interference) does not contribute to the increase of SINR and thus spectral efficiency. The analysis of the saturation point and its variation over the multiple clustering techniques are presented in Section VI-C.

In general, a fully cooperative cell-free distributed network outperforms a scenario with two cells. Nevertheless, When $0.45 \leq \Delta_E = \Delta_G \leq 0.7$ in Fig. 3a, the P-MMSE-E has higher spectral efficiency when $L = 2, S = 1$ than P-MMSE-G when $L = S = 1$. The advantage of using a system with smaller cells and a lower number of antennas per cell N is reflected in the computational cost, this reduction is reflected in Fig. 9 and analysed in Section VI-F, as for the case $L = 2$, $S = 1$ only $N = 32$ antennas are serving a user,

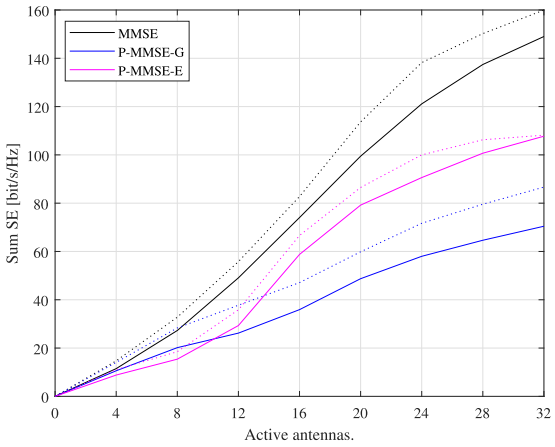

(a) Fully cooperative system ($S = L = 1$). The number of dominant ($\Delta_s = 0.5$) and the number of dominant interferers suppressed $Q_E = Q_G \approx 22$ this corresponds to $\Delta_E = \Delta_G = 0.7$. 11 corresponds to $\Delta_E = \Delta_G = 0.7$

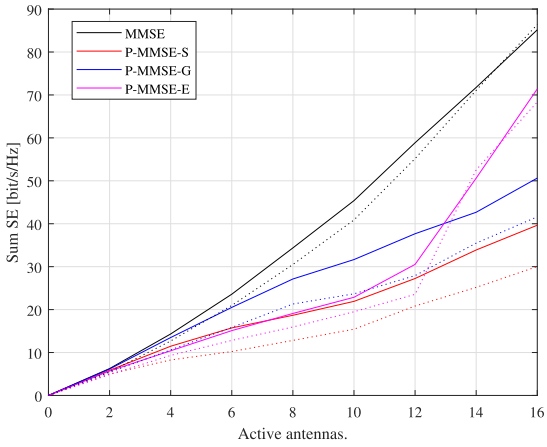

(b) System: $L = 2$ $S = 1$. The set value given by the system for Q_S is 8 or

FIGURE 4. **Variation of the total spectral efficiency (SE) over the number of active antennas (NS_k). Here the total users is $K = 32$. The solid lines are the results based on the massive MIMO experiment and the dotted lines are the results for a WINNER II channel model. The performance of P-MMSE-E increases for a high number of active antennas, while, as it is expected for the remained combining vectors the performance is almost linear to the number of antennas.**

while $L = S = 1$ uses $N = 64$ antennas (not even counting backhauling cost improvements). However, the spectral efficiency performance of those combining vectors in the mentioned range is below the 50% of the optimal MMSE.

Fig. 3b shows the simulation results for the same clustering strategies described above for the model-based WINNER II channel. The spectral efficiency determined with the experimental and modelled channels are similar and have the same trend. Interestingly, for a fully cooperative system ($L = S = 1$), the model-based results are more optimistic than the experimental ones. In contrast with the second clustering strategy ($L = 2$, $S = 1$), where the experimental results outperform the model-based ones, highlighting the fact that the model might underestimate interference or correlation between users. The WINNER II model is one of the few models that allows the estimation of indoor channels, and in terms of spectral efficiency, it performs in close range to the real values obtained by the experiment. Nevertheless, a full analysis of the physical channel characteristics is required to find the similarities and differences with indoor experimental channels.

B. SCALING WITH ACTIVE ANTENNAS

In MIMO systems, the active number of antennas NS, improves the performance of the system, as it is reflected in Fig. 4. This figure depicts the total spectral efficiency when the number of active antennas increases and its effect on all the different MMSE combining vector variations, for a fully cooperative (Fig. 4a) and a two-cell system (Fig. 4b).

Figure 4 portrays the whole range when ${Q_E}^{\text{sat}}$ is selected to reach the best performance ($\Delta_E^{\text{sat}} = 0.7$ as in Fig. 3 for the two-cell system). Therefore, for the fully cooperative system with 64 antennas and 32 users $Q_E \approx 22$. For the two-cell system with 32 antennas and 16 users per cell, ${Q_E}^{\text{sat}} \approx 11$. When the number of antennas decreases while fixing Q_E, we expect a performance degradation as we don't have enough antenna degrees of freedom to suppress all dominant interferers. In the case of a fully cooperative system, Fig. 4a shows that when the number of active antennas increases ($\geq$12) then P-MMSE-E outperforms P-MMSE-G. Besides we can see that in both clustering systems P-MMSE-G increases monotonously with the number of active antennas, similarly to P-MMSE-S.

To endorse our measurement-based analysis and conclusions, we simulated a similar scenario using the WINNER II channel model. The dotted results in Fig. 4 confirm a superior performance for P-MMSE-E when the number of active antennas NS is high enough.

C. P-MMSE-E LIMITATIONS

For the two-cell case presented in Fig. 3 it was visible that the P-MMSE-E achieves a higher spectral efficiency than P-MMSE-G for the same amount of selected dominant interferers ($Q_E = Q_G$), until a saturation point is reached (Q_E^{sat}). This saturation point provides the highest spectral efficiency given by P-MMSE-E for a given number of antennas.

This P-MMSE-E saturation point value depends on the number of serving antennas (NS) and the number of suppressed eigendirections (Q_E). When Q_E exceeds this optimal value or saturation point, more degrees of freedom are used to suppress interference, and cannot be used to improve the signal strength; therefore, the performance of the spectral efficiency will not improve.

Fig. 5 depicts the optimal percentage of eigendirections ($\Delta_E^{sat} \approx Q_E^{sat}(L/K)$) for multiple clustering strategies when $K = 32$ and 8, for experimental and simulation scenarios.

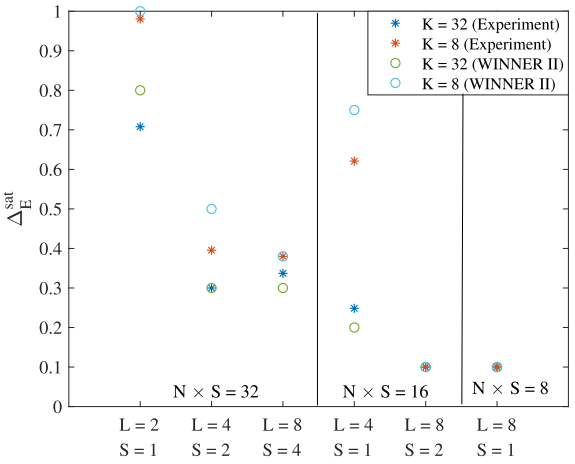

FIGURE 5. Optimal percentage of suppressed Eigendirections $\Delta_E^{sat} \approx Q_E(L/K)$, to achieve the highest spectral efficiency under the use of P-MMSE-G combining vector. The results are presented for multiple network cooperation levels, with $K = 32, 8$.

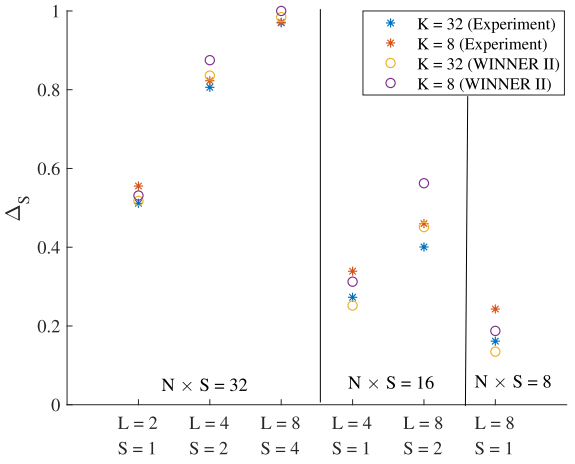

FIGURE 6. Percentage of users that share at least on access point $\Delta_S \approx Q_S(L/K)$ set by the different network cooperation levels, with $K = 32, 8$. Those results are compared between experimental and simulated scenarios.

If the optimal $\Delta_E^{sat} \rightarrow 0$ then the small number of the suppressed eigendirections do not increase the system performance, and P-MMSE-E is not a valid option. This effect occurs in systems with an small number of antennas (NS) and large number of users (K), in our analysis this is the case when $NS < 16$ or when: $L = 4$ $S = 1$, $L = 8$ $S = 2$ and $L = 8$ $S = 1$. On the other hand when the optimal $\Delta_E^{sat} \rightarrow 1$ then P-MMSE-E has a better performance than P-MMSE-G for any given $Q_E = Q_G$ value, this was shown in Fig. 3 when $L = 1$ $S = 1$.

D. ACCESS POINT-BASED INTERFERENCE SUPPRESSION

P-MMSE-S is a special case of P-MMSE-G; therefore, the spectral efficiency of those combining vectors are equal when the number of users allocated to a given set of access points is the same as the number of dominant interferers selected based on channel gain Q_G. That was achieved for $\Delta_G = 0.5$, for $L = 2$ $S = 1$ in Fig. 3. Within the same system P-MMSE-G performs better than P-MMSE-S when $Q_S < Q_G$. Interestingly, one can see in the same figure that the spectral efficiency of P-MMSE-G increases quickly when $Q_S < Q_G$. Although we can not control Q_S, its value is an important parameter to be analysed as it influences P-MMSE-S performance, and it should be high enough when users have more access points in common.

Figure 6 shows the percentage of K users that are suppressed in P-MMSE-S presented as $\Delta_S \approx Q_S(L/K)$, according the different clustering techniques, when $K = 32$ and 8. When $\Delta_S \rightarrow 1$ then the P-MMSE-S performance is similar to MMSE, which occurs when the users share more access points, for scenarios as $L = 4$ $S = 2$ and $L = 8$ $S = 4$. On the other hand when $\Delta_S \rightarrow 0$, P-MMSE-G will achieve a better performance than P-MMSE-S. This occurs when the system is deployed as small cells i.e. $L = 8$ $S = 1$. Interestingly, we see this behaviour in experimental and simulated scenarios as the variation of Δ_S between these two cases is small.

E. SPECTRAL EFFICIENCY PER USER

The sum spectral efficiency per system allows a comparison between the multiple combining vectors and clustering techniques, but this does not give information on the user performance. Fig. 7 and Fig. 8 shows the distribution of the spectral efficiency per user in systems with $K = 32$ and $K = 8$, respectively. The values for Δ_E and Δ_G are set at 0.5, while the values for Δ_S are determined by the clustering scenario, and those values were already presented on Fig. 6. The results are presented as IQR (inter-quartile-range) for a set of $\mathcal{K}$ users in 200 random scenarios. As in Fig. 3, Fig. 4, Fig. 5 and Fig. 6, we saw that the behaviour of experimental and simulation scenarios follow a similar trend and for the sake of simplicity, the results presented in this section correspond to experimental data only.

As expected, the spectral efficiency per user is reduced when the number of total antennas serving each user also reduces; this effect is clearly visible as the mean value (red line in each boxplot) for the MMSE combining vector in Fig. 7 and Fig. 8.

Also, when the number of users is reduced, see Fig. 8, then the overall performance of the system increases due to the high number of serving antennas, regardless of the clustering technique and the combining vectors.

In case of partial interference suppression P-MMSE-S, one clearly sees the impact of cancelling a large percentage of dominant interferers, ($\Delta_S \rightarrow 1$). As a highlight, for $L = 8$ $S = 4$, we see that as the mean value of P-MMSE-S approximates to the mean value of MMSE, as most interference is suppressed, due to a high probability of users sharing multiple access points. The opposite happens in $L = 4$ $S = 1$ and $L = 8$ $S = 1$ (small cells), where the performance of P-MMSE-S (as $\Delta_S \rightarrow 0$) is the lowest in comparison with the remaining combining vectors.

For the case of a controlled interference suppression scenario as PMMSE-E, the access points with a higher number of antennas (N) that suppress a small set of interferes allows

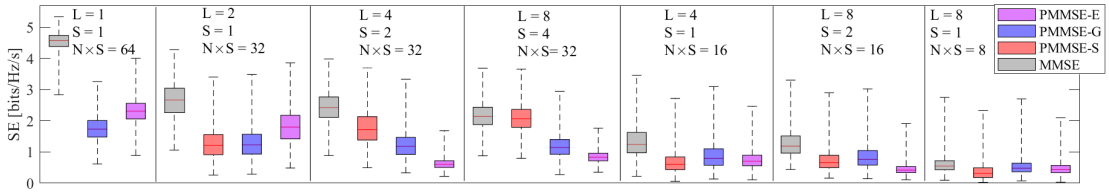

FIGURE 7. Spectral efficiency distribution per users for multiple network cooperation levels and under full and partial interference suppression. Considering a system with $K = 32$ and $\Delta_E = \Delta_G = 0.5$.

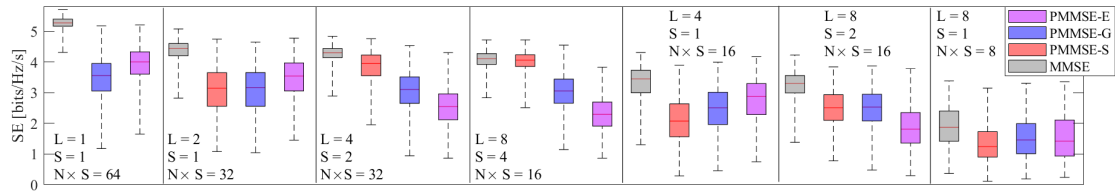

FIGURE 8. Spectral efficiency distribution per users for multiple network cooperation levels and under full and partial interference suppression. Considering a system with $K = 8$ and $\Delta_E = \Delta_G = 0.5$. It is important to note that computational complexity is mainly dominated by the number of active antennas NS. If we compare configurations with similar complexity, then we see that for $NS = 32$ the best topology is $L = 2$, $S = 1$, which means a network-centric clustering. On the other hand, when we are dealing with smaller numbers of active antennas $NS = 16$, the best topology is $L = 8$, $S = 4$, which gives us most degrees of freedom to select those antennas that are best to serve a given user. As L and S are large, we have very user-centric clustering with many degrees of freedom.

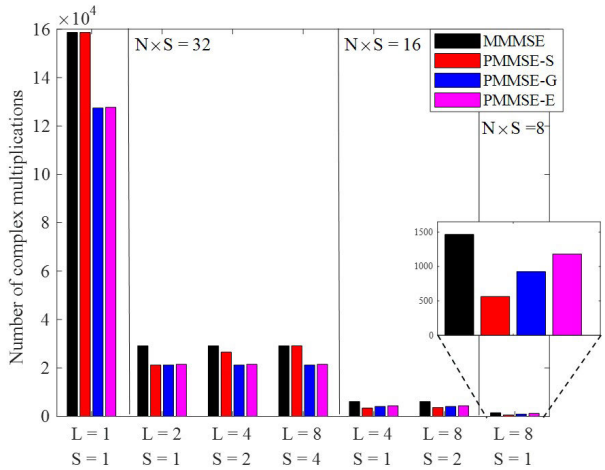

FIGURE 9. Number of complex multiplications per user k for the different combining vectors, under multiple network cooperations. In this case $Q_E = Q_G = 0.5K$ and $K = 32$.

TABLE 4. Standard deviation of the spectral efficiency per user, for difference network cooperation levels, when $K = 32$ and $\Delta_E = \Delta_G = 0.5$.

L	S	N× S	MMSE	PMMSE-S	PMMSE-G	PMMSE-E
1	1	64	0.2966	X	0.3960	0.3878
2	1	32	0.5555	0.4883	0.4868	0.5497
4	2	32	0.4769	0.5539	0.4251	0.1733
8	4	32	0.4208	0.4354	0.3693	0.1926
4	1	16	0.5459	0.3841	0.4798	0.3139
8	2	16	0.4825	0.3787	0.4421	0.1961
8	1	8	0.3522	0.2875	0.3337	0.2487

TABLE 5. Standard deviation of the spectral efficiency per user, for different network cooperation levels, when $K = 8$ and $\Delta_E = \Delta_G = 0.5$.

L	S	N× S	MMSE	PMMSE-S	PMMSE-G	PMMSE-E
1	1	64	0.1801	X	0.6595	0.5764
2	1	32	0.3417	0.7372	0.7391	0.6380
4	2	32	0.2434	0.4904	0.6229	0.6169
8	4	32	0.2698	0.3076	0.5722	0.5567
4	1	16	0.5632	0.7289	0.7364	0.6958
8	2	16	0.4206	0.5760	0.6149	0.7031
8	1	8	0.6516	0.6025	0.6719	0.7508

to reach a higher performance. This is clear when comparing the cases of $L = S = 1$ and $L = 2$ $S = 1$ in Fig. 7 and Fig. 8 (including $L = 4$ $S = 1$).

Another important parameter to analyse is the spectral efficiency fairness per user. Thus, Table 4 and 5 present the standard deviation of the spectral efficiency per user. A smaller standard deviation indicates that there is less variation in spectral efficiency across users. Notice that a full interference suppression (MMSE) does not always guarantee user fairness.

F. COMPUTATIONAL COST PER USER

While a fully-cooperative system ($S = L = 1$) is preferred in terms of spectral efficiency, it will require a huge computational cost as it is presented in Fig. 9. In this figure the values for Δ_E and Δ_G are 0.5, while for Δ_S the values considered are those presented in Fig. 6. As was shown in Table 2, NS has a higher influence in the computational cost than Q. Therefore, in overall to reduce the cost one should consider a lower number of serving antennas. It is important to notice that as Q_E and Q_G are the same but in terms of computational cost the P-MMSE-E requires extra complex multiplications which is more noticeable in an scenario with small cells ($L = 8$ $S = 1$).

VII. CONCLUSION

This work identifies the taxonomy of multiple clustering methods and interference suppression techniques applied to

partial MMSE combining vectors, each of them named in different forms. Therefore a general MMSE combining vector is proposed; this combining vector is versatile enough to adapt to any clustering technique and allows the comparison between multiple dominant interferers suppression methods. To study the different variations of the proposed MMSE the wireless channel was collected in an experimental indoor dense scenario with the aid of the massive MIMO KU Leuven testbed and contrasted with simulation results under a WINNER II channel model.

Based on the simulation and experimental results, we obtained three main conclusions related to interference suppression. First, the P-MMSE-S is viable only when more than one access point serves a user; its performance decreases drastically for a small-cell case scenario.

Second, the P-MMSE-G which uses a channel gain based suppression is the best controllable combining method regardless the clustering methodology, with this combining vector it is possible to achieve an accurate trade-off between spectral efficiency and computational cost.

Third, the proposed P-MMSE-E that relies on the suppression of the interfering eigendirections shows the best spectral efficiency in comparison with the other two partial combining vectors (under the right parameters). These results lead us to the conclusion that the suppression of eigendirections has more impact than the suppression of interference based on channel gain for systems with a higher number of antennas.

In addition, the comparison between experimental and simulated data using the WINNER II channel model, lead us to the conclusion that the simulated channel model shares similar characteristics with the experimental one in terms of spectral efficiency and interference suppression performance.

REFERENCES

[1] T. L. Marzetta, "Noncooperative cellular wireless with unlimited numbers of base station antennas," *IEEE Trans. Wireless Commun.*, vol. 9, no. 11, pp. 3590–3600, Nov. 2010.

[2] T. L. Marzetta and H. Yang, *Fundamentals of Massive MIMO*. Cambridge, U.K.: Cambridge Univ. Press, 2016.

[3] E. Björnson, E. G. Larsson, and M. Debbah, "Massive MIMO for maximal spectral efficiency: How many users and pilots should be allocated?" *IEEE Trans. Wireless Commun.*, vol. 15, no. 2, pp. 1293–1308, Feb. 2016.

[4] C. Shepard, H. Yu, N. Anand, E. Li, T. Marzetta, R. Yang, and L. Zhong, "Argos: Practical many-antenna base stations," in *Proc. 18th Annu. Int. Conf. Mobile Comput. Netw.*, 2012, pp. 53–64.

[5] P. Harris, W. B. Hasan, H. Brice, B. Chitambira, M. Beach, E. Mellios, A. Nix, S. Armour, and A. Doufexi, "An overview of massive MIMO research at the University of Bristol," in *Proc. Radio Propag. Technol. 5G*, Oct. 2016, pp. 1–5.

[6] S. Malkowsky, J. Vieira, L. Liu, P. Harris, K. Nieman, N. Kundargi, I. C. Wong, F. Tufvesson, V. Öwall, and O. Edfors, "The world's first real-time testbed for massive MIMO: Design, implementation, and validation," *IEEE Access*, vol. 5, pp. 9073–9088, 2017.

[7] C.-M. Chen, V. Volskiy, A. Chiumento, L. van der Perre, G. A. E. Vandenbosch, and S. Pollin, "Exploration of user separation capabilities by distributed large antenna arrays," in *Proc. Globecom Workshops (GC Wkshps)*, Dec. 2016, pp. 1–6.

[8] A. P. Guevara, C.-M. Chen, and S. Pollin, "Hardware and spectrum sharing for distributed massive MIMO," in *Proc. Asilomar Conf. Signals, Syst., Comput.*, Oct. 2018, pp. 619–623.

[9] A. P. Guevara and S. Pollin, "Densely deployed indoor massive MIMO experiment: From small cells to spectrum sharing to cooperation," *Sensors*, vol. 21, no. 13, p. 4346, Jun. 2021. [Online]. Available: https://www.mdpi.com/1424-8220/21/13/4346

[10] A. P. Guevara, S. De Bast, and S. Pollin, "Weave and conquer: A measurement-based analysis of dense antenna deployments," in *Proc. IEEE Int. Conf. Commun. (ICC)*, Jun. 2021, pp. 1–6.

[11] A. P. Guevara, S. De Bast, and S. Pollin, "MaMIMO user grouping strategies: How much does it matter?" in *Proc. 53rd Asilomar Conf. Signals, Syst., Comput.*, Nov. 2019, pp. 853–857.

[12] E. Björnson, J. Hoydis, and L. Sanguinetti, "Massive MIMO networks: Spectral, energy, and hardware efficiency," *Found. Trends Signals Process.*, vol. 11, nos. 3–4, pp. 154–655, 2017, doi: 10.1561/2000000093.

[13] E. Björnson, J. Hoydis, and L. Sanguinetti, "Massive MIMO has unlimited capacity," *IEEE Trans. Wireless Commun.*, vol. 17, no. 1, pp. 574–590, Jan. 2018.

[14] A. P. Guevara, C.-M. Chen, and S. Pollin, "Partial multi-cell MMSE vector combining to reduce computational cost for massive MIMO systems," in *Proc. IEEE Int. Conf. Commun. (ICC)*, May 2019, pp. 619–623.

[15] E. Björnson and L. Sanguinetti, "Scalable cell-free massive MIMO systems," *IEEE Trans. Commun.*, vol. 68, no. 7, pp. 4247–4261, Jul. 2020.

[16] X. Li, E. Björnson, E. G. Larsson, S. Zhou, and J. Wang, "A multi-cell MMSE detector for massive MIMO systems and new large system analysis," in *Proc. IEEE Global Commun. Conf. (GLOBECOM)*, Dec. 2015, pp. 1–6.

[17] E. Nayebi, A. Ashikhmin, T. L. Marzetta, and B. D. Rao, "Performance of cell-free massive MIMO systems with MMSE and LSFD receivers," in *Proc. 50th Asilomar Conf. Signals, Syst. Comput.*, Nov. 2016, pp. 203–207.

[18] G. Interdonato, M. Karlsson, E. Björnson, and E. G. Larsson, "Local partial zero-forcing precoding for cell-free massive MIMO," *IEEE Trans. Wireless Commun.*, vol. 19, no. 7, pp. 4758–4774, Jul. 2020.

[19] S. Buzzi, C. D'Andrea, and C. D'Elia, "User-centric cell-free massive MIMO with interference cancellation and local ZF downlink precoding," in *Proc. 15th Int. Symp. Wireless Commun. Syst. (ISWCS)*, Aug. 2018, pp. 1–5.

[20] S. T. Veetil, K. Kuchi, and R. K. Ganti, "Performance of PZF and MMSE receivers in cellular networks with multi-user spatial multiplexing," *IEEE Trans. Wireless Commun.*, vol. 14, no. 9, pp. 4867–4878, Sep. 2015.

[21] A. Ashikhmin, L. Li, and T. L. Marzetta, "Interference reduction in multi-cell massive MIMO systems with large-scale fading precoding," *IEEE Trans. Inf. Theory*, vol. 64, no. 9, pp. 6340–6361, Sep. 2018.

[22] G. Geraci, A. Garcia-Rodriguez, D. López-Pérez, L. G. Giordano, P. Baracca, and H. Claussen, "Indoor massive MIMO deployments for uniformly high wireless capacity," in *Proc. IEEE Wireless Commun. Netw. Conf. (WCNC)*, Apr. 2018, pp. 1–6.

[23] S. Buzzi, C. D'Andrea, A. Zappone, and C. D'Elia, "User-centric 5G cellular networks: Resource allocation and comparison with the cell-free massive MIMO approach," *IEEE Trans. Wireless Commun.*, vol. 19, no. 2, pp. 1250–1264, Feb. 2020.

[24] E. Björnson and L. Sanguinetti, "Making cell-free massive MIMO competitive with MMSE processing and centralized implementation," *IEEE Trans. Wireless Commun.*, vol. 19, no. 1, pp. 77–90, Jan. 2020.

[25] H. Q. Ngo, A. Ashikhmin, H. Yang, E. G. Larsson, and T. L. Marzetta, "Cell-free massive MIMO versus small cells," *IEEE Trans. Wireless Commun.*, vol. 16, no. 3, pp. 1834–1850, Mar. 2017.

[26] T. K. Y. Lo, "Maximum ratio transmission," in *Proc. IEEE Int. Conf. Commun.*, vol. 2, Jun. 1999, pp. 1310–1314.

[27] Q. H. Spencer, A. L. Swindlehurst, and M. Haardt, "Zero-forcing methods for downlink spatial multiplexing in multiuser MIMO channels," *IEEE Trans. Signal Process.*, vol. 52, no. 2, pp. 461–471, Feb. 2004.

[28] X. Li, E. Björnson, S. Zhou, and J. Wang, "Massive MIMO with multi-antenna users: When are additional user antennas beneficial?" in *Proc. 23rd Int. Conf. Telecommun. (ICT)*, May 2016, pp. 1–6.

[29] R. P. Brent, F. T. Luk, and C. Van Loan, "Computation of the singular value decomposition using mesh-connected processors," *J. VLSI Comput. Syst.*, vol. 1, no. 3, pp. 242–270, 1985.

[30] V. Kotzsch, C. Felber, S. Pollin, T. Vermeulen, M. Danneberg, R. Bomfin, W. Liu, I. Moerman, I. Seskar, A. Nahler, F. Paisana, and L. DaSilva. *Orchestration and Reconfiguration Control Architecture, SC2: Definition of Showcases*. Accessed: Nov. 3, 2020 [Online]. Available: https://orca-project.eu/wp-content/uploads/sites/4/2017/01/ORCA_D2.1_Final.pdf

[31] E. Luther. *5G Massive MIMO Testbed: From Theory to Reality*. Accessed: Nov. 3, 2020. [Online]. Available: https://www.ni.com/en-us/innovations/white-papers/14/5g-massive-mimo-testbed–from-theory-to-reality–.html

[32] P. Kyösti, J. Meinilä, L. Hentilä, X. Zhao, T. Jämsä, C. Schneider, M. Narandzić, M. Milojević, A. Hong, J. Ylitalo, V.-M. Holappa, M. Alatossava, B. R, Y. de Jong, and T. Rautiainen. *Winner II Channel Models. D1.1.2 V1.2. IST-4-027756 Winner II*. Accessed: Aug. 21, 2020. [Online]. Available: https://www.cept.org/files/8339/winner2%20-%20final%20report.pdf

ANDREA P. GUEVARA (Graduate Student Member, IEEE) received the B.Sc. degree in electronics and telecommunications from the University of Cuenca, Ecuador, in 2013, and the M.Sc. degree in telecommunications by research from Faculty of Natural and Mathematical Sciences, King's College London, U.K., in 2015. She is currently pursuing the Ph.D. degree with KU Leuven. Her main interests include massive MIMO, infrastructure sharing, precoding, and power leakage. She received the prize for the best academic performance on an M.Sc. degree by research programme from the Faculty of Natural and Mathematical Sciences, King's College London, in 2015.

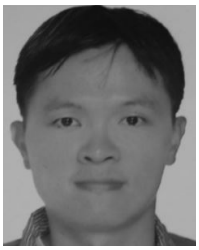

CHENG-MING CHEN received the M.S. degree from the Graduate Institute of Communication Engineering, National Taiwan University (NTU), Taipei City, Taiwan, in 2006, and the Ph.D. degree in electrical engineering from KU Leuven, Belgium, in 2019, investigating distributed massive MIMO systems with software-defined radio. From 2006 to 2011, he has worked on the baseband design of WiMAX and LTE with the Industrial Technology of Research Institute (ITRI), Hsinchu. He was involved in the 802.16m standardization at ITRI. From 2011 to 2015, he was with Broadcom as a Senior System Design Engineer, mainly focused on Wi-Fi receiver bring up.

ALESSANDRO CHIUMENTO (Member, IEEE) received the Ph.D. degree in cellular network management from imec, Leuven, Belgium, in 2015. He subsequently worked as a Postdoctoral Researcher at KU Leuven, Belgium, on massive machine-to-machine communication, channel prediction, very dense networks, and the application of machine learning to theoretical problems in telecommunication and information management. He was a MSCA EDGE Fellow at CONNECT, Trinity College Dublin, and is currently an Assistant Professor with the University of Twente.

SOFIE POLLIN (Senior Member, IEEE) received the Ph.D. degree (Hons.) from KU Leuven, in 2006. From 2006 to 2008, she continued her research on wireless communications, energy-efficient networks, cross-layer design, coexistence, and cognitive radio at UC Berkeley. In 2008, she returned to imec to become the Principal Scientist at the Green Radio Team. She is currently an Associate Professor with the Electrical Engineering Department, KU Leuven. Her research interests include networked systems that require networks that are ever more dense, heterogeneous, battery powered, and spectrum constrained. She is a BAEF Fellow and a Marie Curie Fellow.